Structural Engineering and Mechanics, *Vol. 48, No. 1 (2013) 57-75*
DOI: http://dx.doi.org/10.12989/sem.2013.48.1.057

A numerical investigation of seismic performance of large span single-layer latticed domes with semi-rigid joints

Huidong Zhang[1a] and Qinghua Han[*2]

[1]*School of Civil Engineering, Tianjin Chengjian University, No.26 JinJing Road, XiQing District, Tianjin 300384, China*
[2]*School of Civil Engineering, Tianjin University, No.92 WeiJin Road, NanKai District, Tianjin 300072, China*

(Received February 14, 2012, Revised September 9, 2013, Accepted September 18, 2013)

Abstract. It is still inadequate for investigating the highly nonlinear and complex mechanical behaviors of single-layer latticed domes by only performing a force-based demand-capacity analysis. The energy-based balance method has been largely accepted for assessing the seismic performance of a structure in recent years. The various factors, such as span-to-rise ratio, joint rigidity and damping model, have a remarkable effect on the load-carrying capacity of a single-layer latticed dome. Therefore, it is necessary to determine the maximum load-carrying capacity of a dome under extreme loading conditions. In this paper, a mechanical model for members of the semi-rigidly jointed single-layer latticed domes, which combines fiber section model with semi-rigid connections, is proposed. The static load-carrying capacity and seismic performance on the single-layer latticed domes are evaluated by means of the mechanical model. In these analyses, different geometric parameters, joint rigidities and roof loads are discussed. The buckling behaviors of members and damage distribution of the structure are presented in detail. The sensitivity of dynamic demand parameters of the structures subjected to strong earthquakes to the damping is analyzed. The results are helpful to have a better understanding of the seismic performance of the single-layer latticed domes.

Keywords: single-layer latticed dome; seismic performance; damping; semi-rigid connection; stability

1. Introduction

The single-layer latticed dome is one of the widely used dome systems due to offering a larger space, free design shapes and light weight. The members in a dome mainly carry the axial forces and moments. The mechanical behaviors are highly nonlinear and the load-carrying capacity is affected by various factors, such as geometric shape of a dome, supporting condition, span-to-rise ratio, joint rigidity and damping model (Yuan and Dong 2002, Masayoshi *et al.* 2003). For this reason more attention should be paid to the stability of the system in designing.

Many researchers have investigated the nonlinear behaviors of single-layer latticed domes through both numerical simulations and experiments. The critical load of a single-layer latticed dome could be estimated by means of the results of the buckling theory of a statically equivalent solid shell, by assuming rigid connections between the members (Dulácska and Kollár 2000).

∗Corresponding author, Professor, E-mail: qhhan@tju.edu.cn

http://www.techno-press.org/?journal=sem&subpage=8 ISSN: 1225-4568 (Print), 1598-6217 (Online)

Gioncu (1995) considered that material nonlinearities, whilst often observed in double-layer domes, were not likely to occur in single-layer latticed domes. The effects of geometrical imperfections on the behaviors of single-layer latticed domes are complex and important and the initial imperfections can give rise to an apparent reduction of the axial stiffness of a member. Therefore, the nonlinear buckling behaviors of single-layer latticed domes with geometrical imperfections were studied and an analytical solution was obtained on the basis of a theoretical model proposed by Nie (2003). Bălut and Gioncu (2000) studied the effects of initial imperfections on the behaviors of domes and suggested the use of particular devices for the control of the correct geometry.

However, the behaviors of single-layer latticed domes are greatly affected by the rigidity of the joint, and it is difficult to model. The semi-rigidity of the connections and the geometric imperfections of members leading to the reductions of the critical load of a dome were investigated by Kato *et al.* (1998). Lopez (2007a) studied the nonlinear behaviors of single-layer latticed domes with different geometric parameters and joint rigidities and proposed a new formula for rapidly estimating the buckling loads of the semi-rigidly jointed single-layer latticed domes. Kim *et al.* (2008) investigated experimentally the effects of the various parameters on the flexural performance of the proposed welded jointing system.

In recent years, the researches on dynamic performance of single-layer latticed domes subjected to earthquake loading have been conducted by Kim *et al.* (1997), Li and Shen (2001), Li and Chen (2003), Zhi *et al.* (2007). However, it is still inadequate for investigating the highly nonlinear and complex mechanical behaviors of the single-layer latticed domes. In the last few years, the energy-based analysis has been largely accepted for assessing the seismic capacity of existing structures (Akiyama 2010, Gaetano 2001, Zhang and Wang 2012). The use of the energy-based analysis for seismic design is more realistic and rational. However, the seismic researches based on energy balance concept on single-layer latticed domes are less found in previous papers.

An ultimate limit state analysis of a single-layer latticed dome subjected to earthquake ground motions is necessary to determine the maximum dynamic load-carrying capacity. In the present paper, a mechanical model for members in semi-rigidly jointed single-layer latticed domes is proposed. The static load-carrying capacity and energy-based seismic performance at the ultimate limit state are investigated by means of the proposed model, in which the material and geometric nonlinearities are taken into account. Finally, the sensitivity of the seismic demands to the damping is assessed.

2. Elasto-plastic mechanical model of a member

2.1 Joint-tube-joint model

A member in the single-layer latticed dome is connected to solid steel balls by means of high strength bolts, which are tightened by two nuts. The single-layer latticed dome is regarded as being composed of members and joints. The detailed model is illustrated in Fig. 1(a).

A member consists of a tube with joints at ends, which is called as a joint-tube-joint group. In the nonlinearly numerical analysis, the following approximations are proposed for the model. The stiffness of the balls is considered to be infinite and the bolt is an elasto-plastic cylinder located between the tube and the ball, as illustrated in Fig. 1(b). The two parts are considered as an integrated component having the semi-rigid joint behaviors with the bending capacity. The tube is

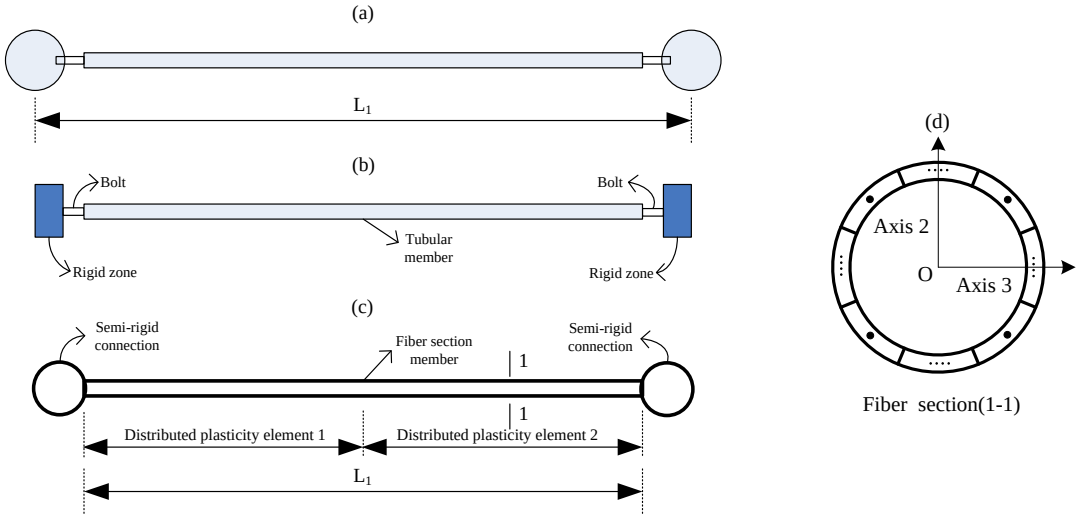

Fig. 1 Mechanical model of joint-tube-joint group and fiber cross-section

modeled with fiber section model. In such a case, the distributed plasticity of a member is taken into account. The local buckling of a member in a single-layer latticed dome generally occurs at its middle. In order to capture the nonlinear behavior the use of two elements per physical member is enough. The mechanical model of the joint-tube-joint group is shown in Fig. 1(c). The section fibers are shown in Fig. 1(d).

Geometric and material nonlinearities are taken into account in the mechanical model. The elasto-plastic behaviors in the model are modeled in two types: (1) fiber elements, it is modeled by accounting for spread-of-plasticity effects in the section and along the member and (2) semi-rigid connections, the inelastic behaviors are concentrated at ends of a member. The proposed model can capture the spreading of plasticity with computational efficiency and the necessary degree of accuracy.

2.2 Modeling of a joint

Joint rigidity is a particularly key factor to the behaviors of single-layer latticed domes, whose flexibility often makes them unsuitable for spanning large distance. There were numerous studies on semi-rigid connections in previous literatures (Kato *et al.* 1998, Hiyama *et al.* 2000). The joint was modeled as a rotational spring component in these studies, and the properties of the spring component were considered to be elasto-plastic, while the tube was regarded as an elastic one.

The mechanical behaviors of semi-rigid joints are described by means of moment-rotation curve. In the present paper, the M-θ curve is obtained from the previous literature. Here, it is assumed that the axial force has no effect on the bending capacity of semi-rigid connection due to the small length of the bolt. The bending behavior about axis 2 is considered to be elastic and the strength loss in one direction of axis 3 causes the same amount of strength loss in the opposite direction. The effect of strength loss is illustrated in Fig. 2 (CSI 2006).

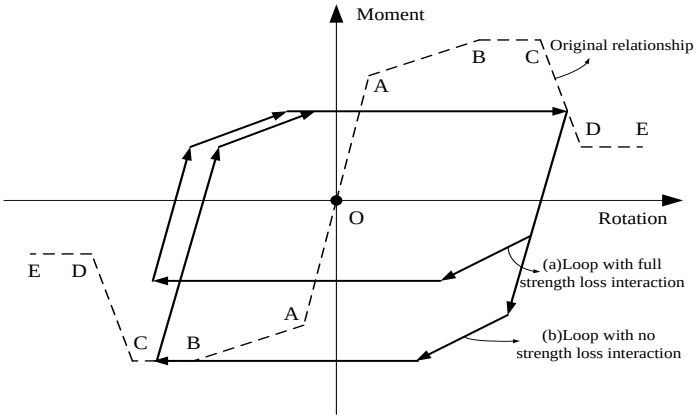

Fig. 2 Loop with different strength loss interaction (CSI 2006)

2.3 P-M-M interaction for fiber section element

The members in single-layer latticed domes subjected to strong earthquakes are simultaneously subjected to both axial force and moments. The axial force usually reduces the bending capacity of a member. Therefore, the combined effect due to *P-M-M* interaction should be taken into account. The fiber section model can well consider the effect. The shear and torsion of a section are assumed to be elastic in this paper. The equations of the yield surface are as follows (El-Tawil and Deierlein 2001a, b). In each *P-M* plane (*P-M*$_2$ and *P-M*$_3$)

$$f_{pm} = (P / P_{y0})^{\alpha} + (M / M_{y0})^{\beta} \tag{1}$$

where f_{pm} = yield function value, =1.0 for yield, P = axial force, M = bending moment, P_{y0} = yield force at M = 0, and M_{y0} = yield moment at P = 0. The effects of the exponents α and β on *P-M* curves are illustrated in Fig. 3. For any value of P, Eq. (1) defines the M value at which yield occurs, in both the *P-M*$_2$ and *P-M*$_3$ planes.

The yield function in the M_2-M_3 plane is then

$$f_{mm} = (M_2 / M_{yP2})^{\gamma} + (M_3 / M_{yP3})^{\gamma} \tag{2}$$

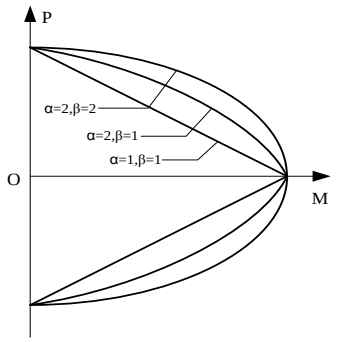

Fig. 3 The yield surfaces in *P-M* interaction

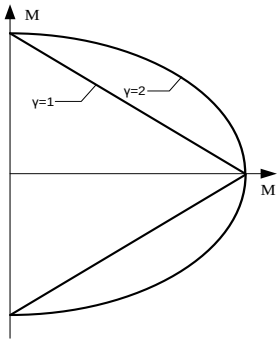

Fig. 4 The yield surfaces in *M-M* interaction

where f_{mm} = yield function value, = 1.0 for yield, M_2 and M_3 = bending moments, M_{yP2} = yield moment at M_3 = 0, and M_{yP3} = yield moment at M_2 = 0. The effect of the exponent γ on *M-M* curves is illustrated in Fig. 4.

3. Discussion on damping in a single-layer latticed dome

The damping is a significant property in the design of structures, especially, in problems involving mechanical resonance and fatigue under cyclic stress. In general, it was difficult to quantify all damping sources in a dome, such as hysteresis, friction at joints and boundary effects, etc.

The viscous damping model is commonly used in dynamic analysis, and in this model the damping is associated with the vibration reduction through energy dissipation. The available sources of energy dissipations in a structure require to be carefully considered and whether these are captured in dynamic analysis. For instance, fiber-type component models, due to capturing the initiation and spread of yielding through the cross section and along the member, will tend to describe the hysteretic energy dissipation at small deformation levels than lumped plasticity hinge models (NEHRP 2010).

Because the damping is difficult to quantify, the experiment method is used to determine the damping characteristics of a structure. For damping models, the complex stiffness damping model is a good alternative (Clough and Penzien 1995). At present there is no clear consensus as to how to resolve damping issues. Therefore, the assessment of the sensitivity of the dynamic demands to the damping is necessary.

In the paper, the classical Rayleigh damping model is used, but it is modified for the dynamic analysis. As a structure is within the plastic range, its effective vibration periods increase. A ductility ratio of n corresponds roughly to a period increase of $n^{0.5}$. The mass and stiffness damping coefficients, α_m and β_k, in Rayleigh damping model can be defined by providing a percentage of critical damping at two different periods of vibration. Reasonable periods to specify these damping values are $0.2T_1$ and $1.5T_1$, where T_1 is the fundamental period of vibration of a structure (NEHRP 2010). Based on observations and guidance in various documents (Charney and McNamara 2008, Charney 2008), it is suggested to specify the equivalent viscous damping ratios in the range of 1% to 5% of critical damping over the range of periods from $0.2T_1$ to $1.5T_1$.

4. Numerical models

The single-layer latticed dome with a span of D = 60m and the ratios of D/H = 4, 5 and 6 is shown in Fig. 5. The tubular section sizes are listed in Table 1.

The yield stress, ultimate stress and strain and Young's modulus of material are set at f_y = 207*MPa*, f_u = 320*MPa*, ε_u = 0.15 and E = 2*10^11*N/m^2*, respectively. The σ-ε curve of material

Table 1 Cross-sections of members

Ridge member	Hoop member	Diagonal member
Φ=152; *t*=5.5mm	Φ=152; *t*=5.5mm	Φ=146; *t*=5mm

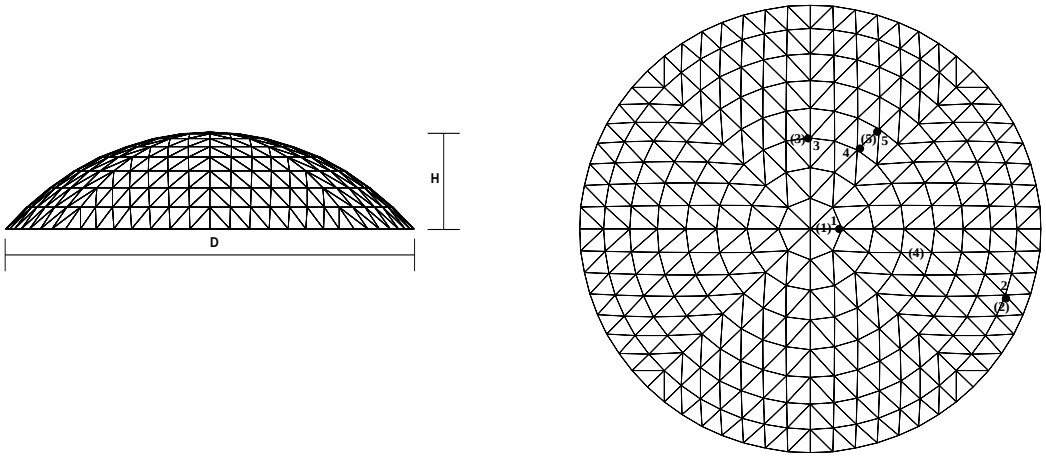

Fig. 5 Single-layer latticed dome model

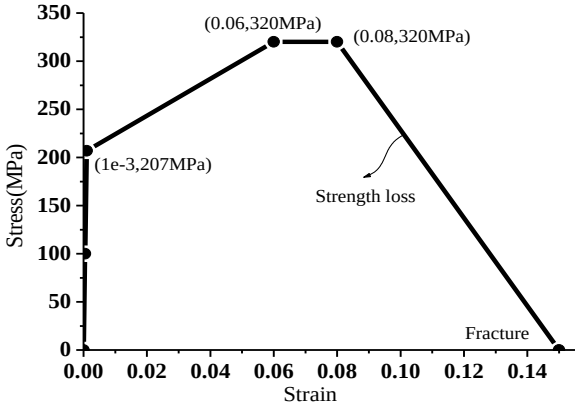

Fig. 6 σ-ε curve of material

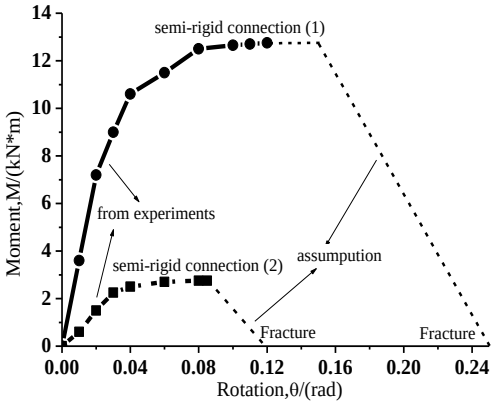

Fig. 7 M-θ curves of semi-rigid joint

with strength loss is shown in Fig. 6. Two M-θ curves for semi-rigid connections in the single-layer latticed dome, which are from the experiment results (Fan *et al.* 2009), are presented in Fig. 7. The strength loss and fracture properties are considered and the ultimate rotations of 0.25 *rad* and 0.12 *rad* are assumed for semi-rigid connection (1) and (2), respectively.

The cross-section of tube is divided into 8 fibers, as shown in Fig. 8. Fig. 9 shows the moment-curvature curves of cross-sections under different axial force levels, which are obtained by performing a section analysis with UCFyber software (Chadwell 1998). UCFyber is a fully interactive software for analyzing moment-curvature and axial force-moment interactions for concrete, steel and composite structural cross sections (even with holes) with nonlinear materials.
The nonlinear time history analyses are carried out by means of the Northridge (1994) and Kobe (1995) ground motion records that are considered as the representatives of many ground motions. These ground motions and different roof loads applied to joints of the structure are shown in Table 2. These analyses are carried out in *Perform 3D* program. The damping ratio is set at 3% for both $0.2T_1$ and $1.5T_1$ in the ultimate limit state analyses. In these analyses, the gravity loads are applied first and then hold constant while the ground motions are applied.

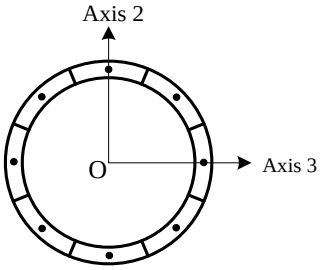

Fig. 8 Fiber cross-section

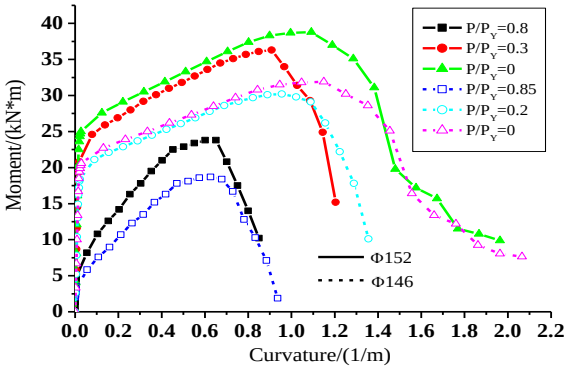

Fig. 9 *M-C* curves under different axial force levels

Table 2 Earthquake ground motions and roof loads

Earthquakes	Northridge (1994)			Kobe (1995)		
	E-W, *PGA*	N-S, *PGA*	UP, *PGA*	E-W, *PGA*	N-S, *PGA*	UP, *PGA*
	0.5165g	0.4158g	0.3265g	0.6934g	0.6936g	0.4333g
Roof load kg/m^2	60,120,180					

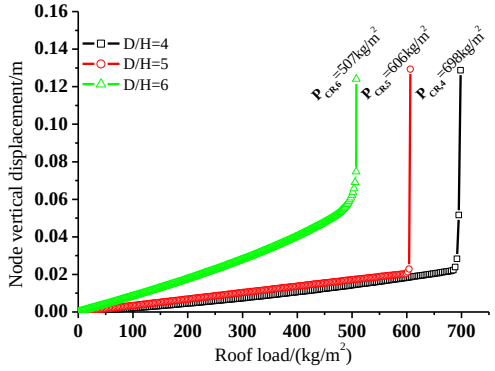

(a) Semi-rigid connection (1)

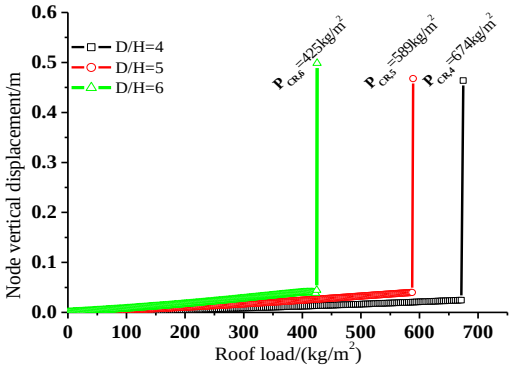

(b) Semi-rigid connection (2)

Fig. 10 Load-displacement curves under vertical static load

5. Results

5.1 Effects of joint rigidity and span-to-rise ratios on static stability

In the static load-deformation curve of a single-layer latticed dome, the first upper ultimate point is most meaningful for practical design, which is far higher than others, and the structure completely loses its stability in case of exceeding the point.

Fig. 10 shows the load-deformation curves of the domes. A buckling criteria based on the structural response was proposed by Budiansky and Roth (1962), called *B-R* criteria, which meant that the buckling occured when a small increase of load led to a suddenly large increase of displacement of a node. According to the criteria and curves, the critical loads, P_{cr}, of the

structures are obtained. When the semi-rigid connection (1) is used for the joint bending performance, these loads are 698kg/m^2, 606kg/m^2 and 507kg/m^2 for D/H = 4,5 and 6, respectively; when the semi-rigid connection (2) is used, these values are 674 kg/m^2, 589 kg/m^2 and 425 kg/m^2, respectively. It shows that the load-carrying capacity of the structure greatly decreases with the increase of the ratio, D/H; while it increases with the increase of joint rigidity, especially for the structure with larger span-to-rise ratio, such as D/H = 6. In these analyses, it is found that the instability of the structure begins with a joint of a ridge member, where there is a large local concave and then some joints near the joint begin to lose stability; finally, the entire structure suddenly loses the load-carrying capacity.

5.2 Energy components at the ultimate limit state only under vertical ground motions

For ordinary buildings, the horizontal response is dominantly governed by the first vibration mode and the vertical earthquake component is not applied to structures in dynamic analysis. However, the vertical earthquake component has the dominant effect on large-span single-layerlatticed domes and should be specially considered (Moghaddam 2000). In previous literatures, the force-based analysis was carried out for investigating the single-layer latticed domes. However, new trends in the seismic design methodologies are oriented to the definition of performance-based methods for the design of new facilities and for the assessment of the seismic capacity of existing facilities (Gaetano 2001). In this paper the energy-based balance analysis is conducted. The relative input energy, E_I, hysteretic energy, E_h, and viscous damping energy, E_ξ, are the key indicators in the energy balance method. The first indicator, E_I, represents the energy intensity of a ground motion imparting to a structure and the latter two indicators, E_h and E_ξ, represent energy dissipation capacity by hysteretic action and damping in a structure.

The energy components have the following approximate relationship at the end of an earthquake

$$E_\xi + E_h \approx E_I \tag{3}$$

The damage potential is associated with the maximum hysteretic energy demand during an excitation. Likewise, the hysteretic energy value represents the degree of damage of a structure subjected to a ground motion. In order to describe the indicators, Akiyama (2010) expressed E_I in terms of the equivalent pseudo-velocity, V_E, as following

$$V_E = \sqrt{2E_I / M} \tag{4}$$

where E_I = input energy; M = total mass. The equivalent pseudo-velocities of other energy components can also be written as the above expression. These parameters can be used for design purposes.

The acceleration values of the vertical ground motion component are multiplied by a scaling factor, which increases until the structure subjected to the scaled ground motion nearly collapse, and the case is defined as the ultimate limit state in this paper. The energy components at the ultimate limit state and their equivalent pseudo-velocities are shown in Tables 3 and 4, where $R_{m,y}$ and $R_{N,y}$ are the ratios of yielding members to total members and yielding joints to total joints, respectively.

These demands, such as the input energy, hysteretic energy, their equivalent pseudo-velocities

Table 3 Energy components under Northridge ground motion (Roof load = 120kg/m^2)

D/H	Connection	E_I (*kN*m*)	E_h (*kN*m*)	E_h/E_I	$R_{m,y}$	$R_{N,y}$	V_E	V_h
4	(1)	861.9	251.9	0.29	39%	0	2.0	1.1
	(2)	447.5	59.5	0.13	19%	0	1.45	0.53
5	(1)	149.2	37.4	0.25	4%	0	0.87	0.44
	(2)	97.9	12.1	0.12	2%	0	0.7	0.25
6	(1)	67.5	0	0	0	0	0.6	0
	(2)	32.6	0	0	0	0	0.42	0

Table 4 Energy components under Kobe ground motion (*D/H* = 5)

Connection	Load (kg/m^2)	E_I (*kN*m*)	E_h (*kN*m*)	E_h/E_I	$R_{m,y}$	$R_{N,y}$	V_E	V_h
(1)	60	109.1	24.7	0.23	3%	0	1.05	0.5
	120	101.5	10.9	0.11	2%	0	0.72	0.24
	180	80.9	5.2	0.06	2%	0	0.52	0.13
(2)	60	79.3	0	0	0	0	0.9	0
	120	70.5	0	0	0	0	0.6	0
	180	65	0	0	0	0	0.47	0

and damage ratios of the structure, remarkably decrease with the increase of the ratio, *D/H*. When the ratio is larger, for example, *D/H* = 6, the elastic instability is the only failure mode and all members in the structure do not yield.

The semi-rigid joint stiffness has a significant effect on these demand parameters. The demands remarkably decrease with the reduction of joint stiffness. The decrease of joint rigidity will accelerate the instability of the structure, and furthermore, the instability tends to be an elastic one. Through Table 4, it is found that these values obviously decrease with the increase of the roof load for the structure with the span-to-rise ratio, *D/H* = 5.

5.3 Behaviors of domes subjected to multidimensional earthquake loads

The following contents show the nonlinear mechanical behaviors of the structure with *D/H*=5 and roof load 120kg/m^2 at the ultimate limit state under three dimensional earthquake loads.

5.3.1 Energy components

The input energy components become gradually steady after reaching the maximum value, while the hysteretic energy components continuously increase, which reach the maximum values at the end of earthquakes. But for the input energy components or the hysteretic energy components, these dynamic demands are remarkably different at the ultimate limit state. The difference is caused by the dynamic properties of a structure and the characteristics of ground motions. The ultimate input energy components are 544*kN*m* and 260*kN*m* under the two ground motions when the semi-rigid connection (1) is used, while these values are 366*kN*m* and

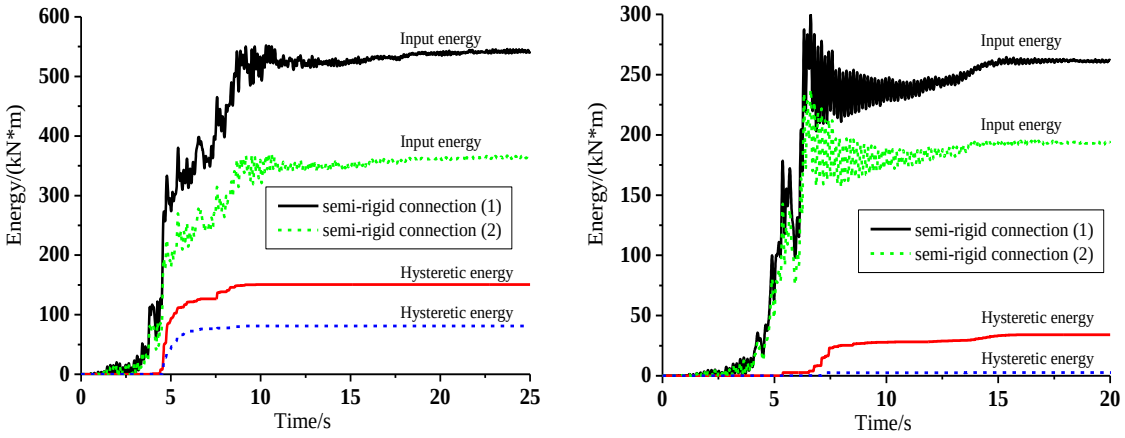

(a) Northridge (1994) (b) Kobe (1995)

Fig. 11 Energy components of structure

193*kN*m* for the semi-rigid connection (2). The hysteretic energy components are 150*kN*m* and 33*kN*m* for the semi-rigid connection (1) and 80*kN*m* and 3*kN*m* with the semi-rigid connection (2). The hysteretic energy ratios, E_h/E_I, are less than 30% under Northridge and Kobe earthquakes. Compared to ordinary buildings, in which the hysteretic energy ratios can reach 50%-70% at the ultimate limit state (Zhang and Wang 2012), the hysteretic energy demands of single-layer latticed domes are smaller. Therefore, according to Eq. (3), the viscous damping is the main energy dissipation source in a single-layer latticed dome.

The semi-rigid joint rigidity has a considerable effect on the hysteretic energy dissipation capacity and the input and hysteretic energy components increase with the increase of joint rigidity. Evidently, for the semi-rigidly jointed single-layer latticed domes, the hysteretic energy dissipation capacity due to members or joints yielding is of lack and the ductility is relatively low.

5.3.2 Damage distribution

The damage distribution can exhibit the relatively weak part in a structure subjected to ground motions, it is useful for modifying the tentative design. The damage distributions of the single-layer latticed domes at the ultimate limit state are shown in Fig. 12 and Fig. 13 and it is found that the damage distributions are different under different excitations. Generally, the structure easily loses the stability under Kobe ground motion.

The damage of the structure subjected to Northridge ground motion mainly concentrates on the hoop members located on almost every ring except the outside first ring, several ridge members at top and a few of diagonal members. In the structure, there are several joints exceeding the yield moment. When the structure is subjected to the Kobe ground motion, some diagonal members have been damaged and very few of joints yield, and the damage degree of the structure is slighter than that of the one subjected to Northridge ground motion. The reason is that the serious local failure of a few members early occurs under Kobe ground motion, which results in the reduction of load carrying capacity of the structure, the plasticity capacity of most members is not fully developed in this case.

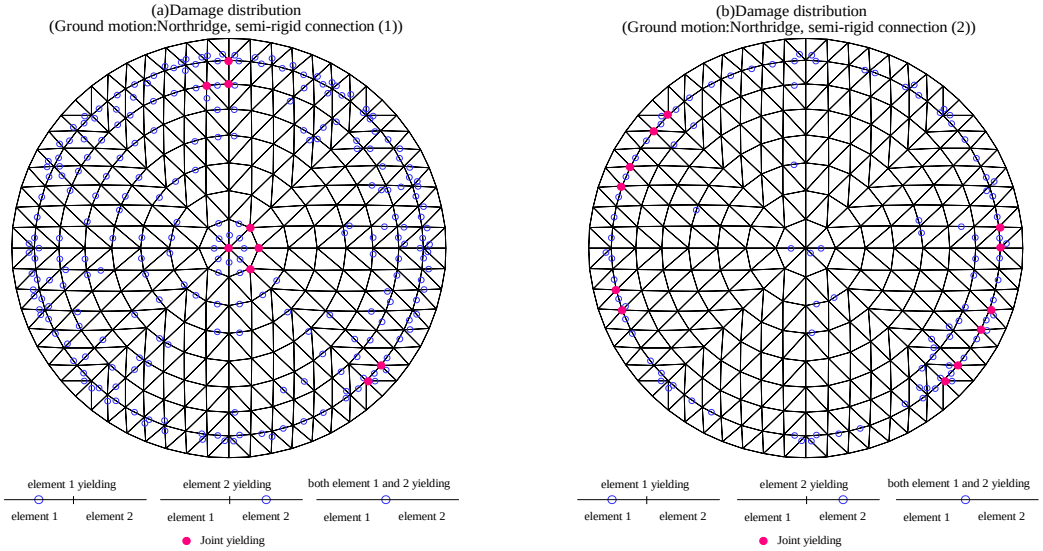

(a) Semi-rigid connection (1) (b) Semi-rigid connection (2)

Fig. 12 Damage distribution of structures subjected to Northridge ground motion

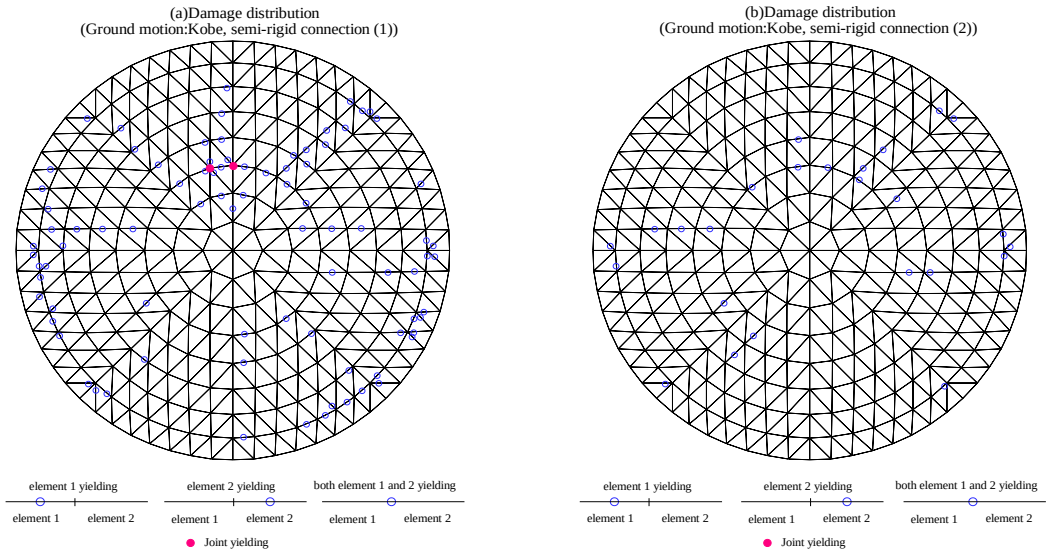

(a) Semi-rigid connection (1) (b) Semi-rigid connection (2)

Fig. 13 Damage distribution of structures subjected to Kobe ground motion

Semi-rigid connection rigidity has a significant effect on the load-carrying capacity and damage in the structure. When the structures are subjected to Northridge ground motion, the ratios of yielding members to total members are about 24% for semi-rigid connection (1) and 9% for semi-rigid connection (2), while the ratios under Kobe ground motion are 8% and 2.5%, respectively. In general, the larger the rigidity of joint is, the more hysteretic energy is and the better the stability is.

The failure modes of the single-layer latticed dome reaching the ultimate limit state mainly include three cases: (a) plastic failure, (b) elasto-plastic failure and (c) elastic instability. In plastic failure mode, it means that the plasticity of a lot of members can be fully developed and some joints reach the yielding moment, the ratio, E_h/E_I, has a relatively larger value, as shown in Fig. 12(a) and 12(b). In elasto-plastic failure mode, it means that a few members reach the yielding strength and very few joints reach the yielding moment, the serious local failure results in the structural instability and the ratio, E_h/E_I, has a very small value, as shown in Fig. 13(a). In the elastic instability mode, it means that almost all of members and joints are elastic when the structure loses the global stability, and the ratio, E_h/E_I, is close to zero, as shown in Fig. 13(b).

5.3.3 Dynamic behaviors

Dynamic response

The dynamic demands of some members are shown in Figs. 14 to 17. It can be observed that the displacements of the members begin to nonlinearly increase, the instability occurs at their middle, and the members continue to work at new balance position, as shown in Fig.14(a) to Fig.17(a). The instability processes of members subjected to the interaction between the axial force and moments are also captured by the nonlinear behaviors of sections, as shown in Figs. 14(b)-17(b) and Figs. 14(c)-17(c). After the buckling of members, the structure has a redistribution of the internal forces and some joints begin to yield due to the bending, as shown in Figs. 14(d)-16(d), indicating that the failure of members is ahead of that of joints.

Failure modes of a tube

According to the results in this paper, it is found that the moment, M_2, is very small. Evidently,

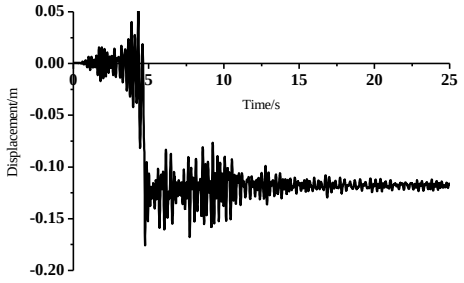

(a) Vertical displacement at middle of member (1)

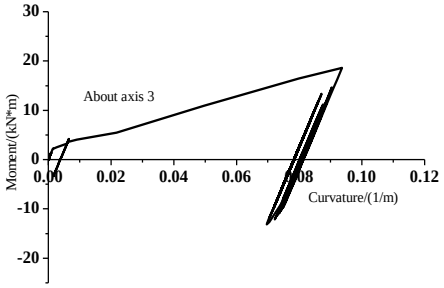

(b) Moment-Curvature at middle of member (1)

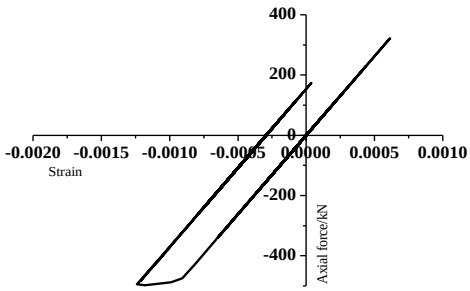

(c) Axial force and strain at middle of member (1)

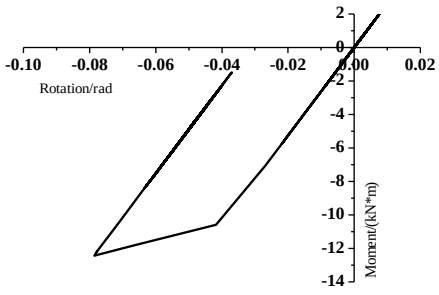

(d) Moment-Rotation curve of joint 1

Fig. 14 Force-Deformation curves of member (1) and joint 1 (Northridge, Semi-rigid connection (1))

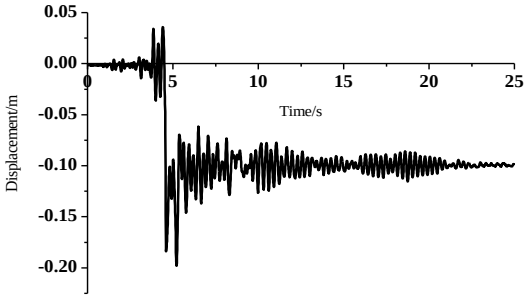

(a) Vertical displacement at middle of member (2)

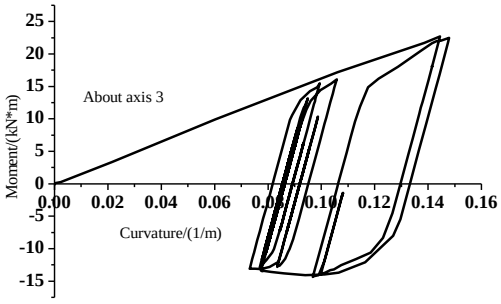

(b) Moment-Curvature at middle of member (2)

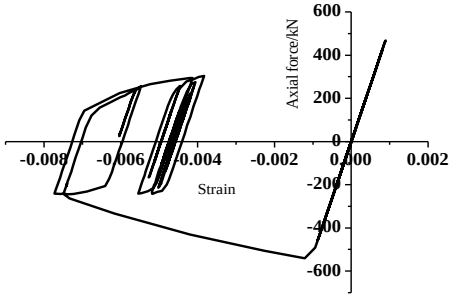

(c) Axial force and strain at middle of member (2)

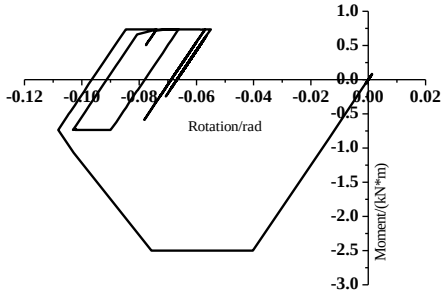

(d) Moment-Rotation curve of joint 2

Fig. 15 Force-Deformation curves of member (2) and joint 2 (Northridge, Semi-rigid connection (2))

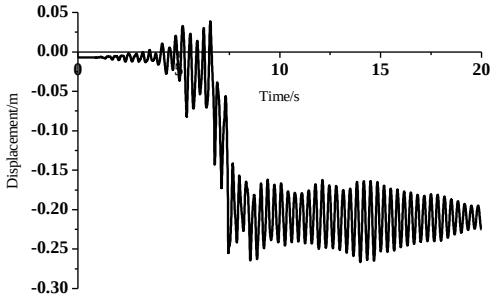

(a) Vertical displacement at middle of member (3)

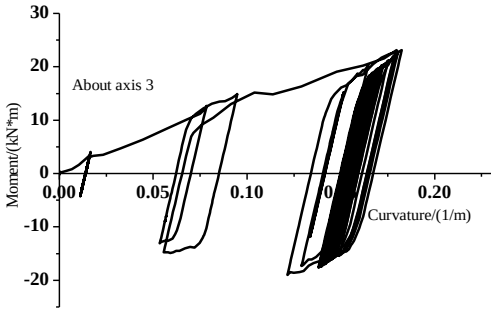

(b) Moment-Curvature at middle of member (3)

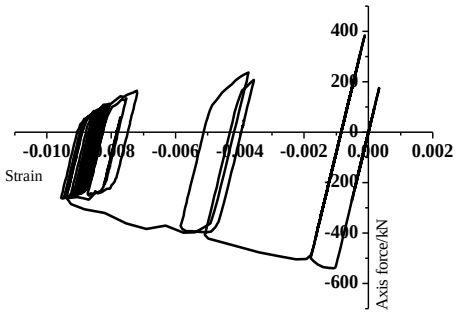

(c) Axial force and strain at middle of member (3)

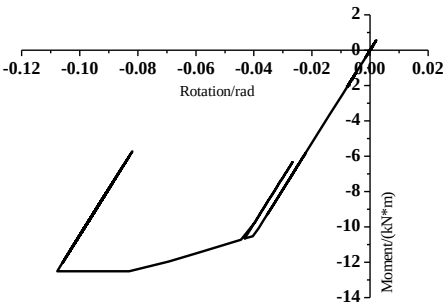

(d) Moment-Rotation curve of joint 3

Fig. 16 Force-Deformation curves of member (3) and joint 3 (Kobe, Semi-rigid connection (1))

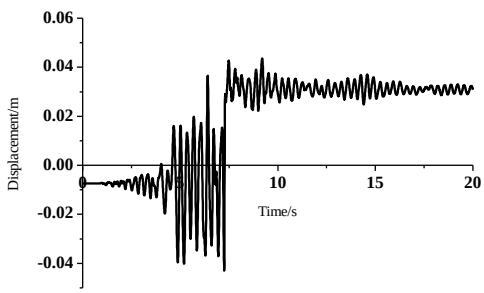

(a) Vertical displacement at middle of member (4)

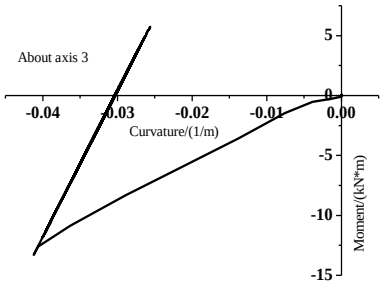

(b) Moment-Curvature at middle of member (4)

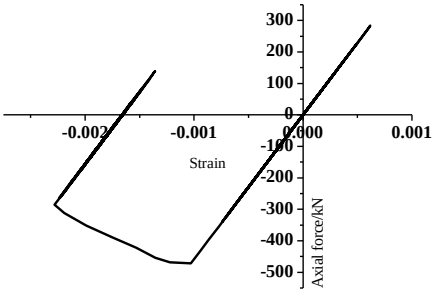

(c) Axial force and strain at middle of member (4)

Fig. 17 Force-Deformation curves of member (4) (Kobe, Semi-rigid connection (2))

the members lose the stability due to the compression-bending buckling in 1-3 plane. The failure mode of a member with ϕ = 152mm, t = 5.5mm and length 5m is further investigated with shell elements. The member is fixed at both ends. If ignoring the small moment, M_2, the member is a unidirectional eccentric compression member, as shown in Fig. 18(a). In this analysis, the axial force is kept as a constant while an increasing rotation is applied, and the transverse gravity of the member is also taken into account.

When applying the rotation, the member will first be subjected to a global elastic deformation. After the elastic limit of the tube material has been reached the tube will have a permanent deformation after unloading, but the deformation will still be global. If the rotation is further increased, the local buckling occurs and the global deformation will continue, but most of the applied bending energy will be accumulated in the local buckling region until the ultimate moment capacity is reached. At this point, a geometrical collapse will occur if the rotation is additionally increased. The collapse mode is shown in Fig. 18(b), which is the most common failure of a member in single-layer latticed domes before the structures lose the global stability (Lopez 2007b).

The moment-rotation relationships of the member under different axial compression forces are illustrated in Fig. 18(c). It can be seen that the axial compression force significantly reduces the resistance-bending capacity of the member and results in a low ductility. After reaching the maximum moment, the load-carrying capacity rapidly decreases and the elastic limit is far not reached. For a pure bending case, the moment-rotation relationship taking into account material and geometric nonlinearities consists of 4 stages: (I) elastic stage, (II) elasto-plastic stage, (III) plastic stage and (IV) collapse stage. If the joint between members is considered ideally pinned the member is only subjected to the axial force, P, and transverse gravity. The failure mode is shown

in Fig. 19(a). With the increase of the axial force, when the elastic limit has been reached the tube begins to bend, accompanied with the stress increasing, and the local buckling occurs. Finally, the member loses the load-carrying capacity. The force-deformation curve is illustrated in Fig. 19(b). However, for the members with larger slenderness ratio, they easily lose the stability before the elastic limit is reached.

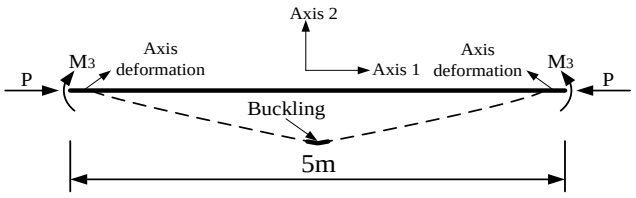

(a) Instability under P and M

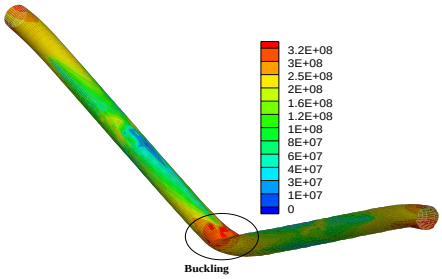

(b) Buckling mode

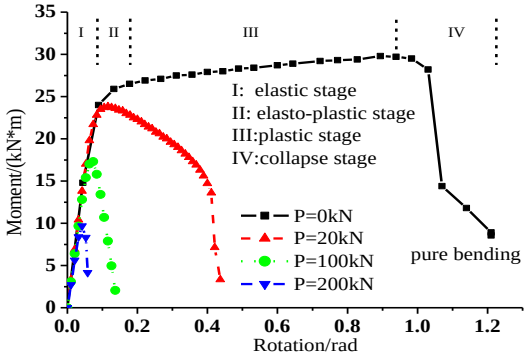

(c) Moment-rotation under different axial force levels

Fig. 18 Buckling of pipe under the interaction between P and M

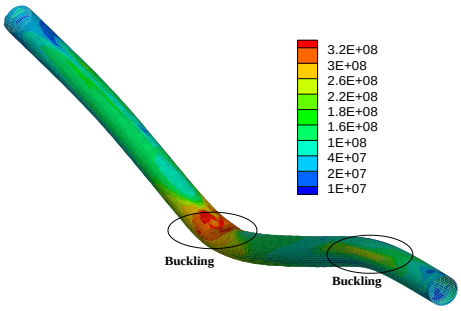

(a) Buckling mode

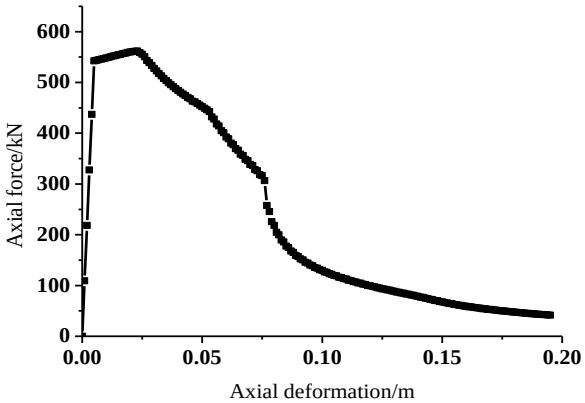

(b) Curve of the axial force and deformation

Fig. 19 Buckling of pipe under the axial force, P

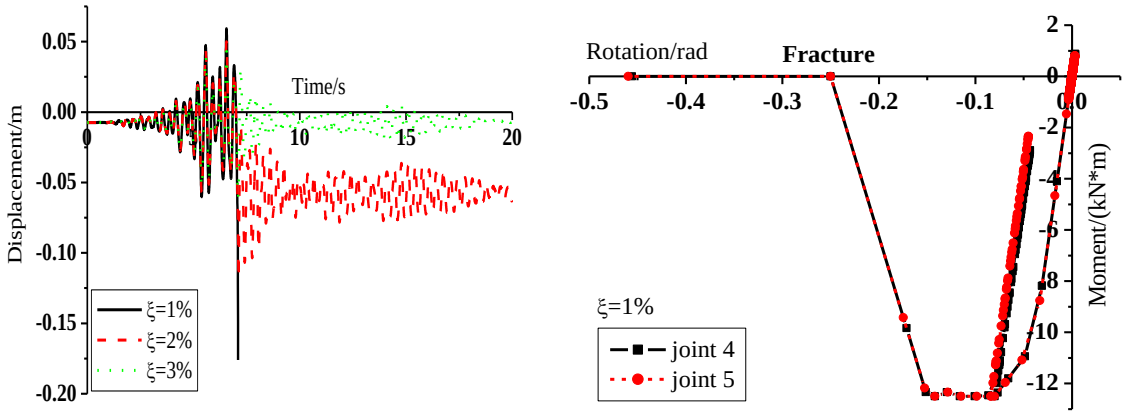

(a) Vertical displacement at middle of member (5) (b) Moment-Rotation curves of joint 4 and 5

Fig. 20 Effect of damping on dynamic demands

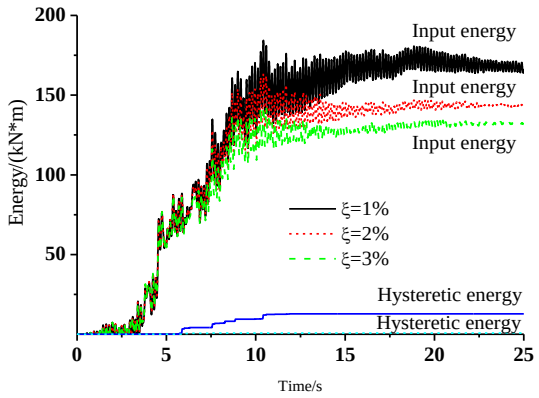

Fig. 21 Energy components under Northridge ground motion

5.4 Sensitivity of dynamic demands to damping

The sensitivity of the dynamic demands to the damping is investigated in this paper. The structure with *D/H* = 5 and roof load 120kg/m^2 under three dimensional seismic loads (scale factor = 1) in Table 2 is discussed.

5.4.1 Response parameters

The displacements at middle of member (5) and moment-rotation curves of joint 4 and 5 under Kobe ground motion are shown in Fig. 20(a). When the damping ratio is set at 1% the displacement response is divergent and the structure fails at 7.5s; at the same time, the joints are fractured, as illustrated in Fig. 20(b). If the damping ratio of 2% is selected, it can be found that the member loses the stability and the maximum displacement reaches 0.12m, while the displacement reaches 0.06m in the case of the damping ratio of 3%. But the joints in the two cases still are elastic. Therefore, the selection of the damping ratio is a key factor for obtaining the

reliable demands in dynamic analysis. The increase of damping has an inhibited effect on the response and it is favorable for the stability.

5.4.2 Energy parameters

The seismic input energy imparted to a structure is dissipated by hysteretic behavior and other non-yielding mechanisms usually represented by the equivalent viscous damping. It is generally realized that there is a strong correlation between the energy dissipated by hysteretic action and the induced level of damage.

The energy components under Northridge ground motion are illustrated as Fig. 21. It can be observed that the energy components, such as the input and hysteretic energy, increase with the decrease of the damping ratio. The ratios, E_h/E_I, are 8%, 1% and 0, respectively. It is clear that the effect of the selection of the damping ratio on these dynamic demand predictions is remarkable. The increase of damping has an inhibited effect on the damage.

6. Conclusions

In this study, a mechanical model combining fiber section model with semi-rigid joints for members in a single-layer latticed dome is proposed, which can give a more exact analysis for the semi-rigidly jointed single-layer latticed domes. The energy-based seismic analysis is included in this work, which enables engineers deeply to understand the seismic performance of this kind of structures from another point of view. The following conclusions can be drawn for design purposes.

• The span-to-rise ratio, roof load and joint rigidity have a significant effect on the static and dynamic load-carrying capacities, which decrease with the increase of span-rise ratio and roof load and increase with the increase of joint connection rigidity. When the span-to-rise ratio is larger or joint rigidity is lesser the elastic instability tends to occur in a single-layer latticed dome. It is also found that the failure of a member is ahead of those of joints.

• From the point of view of the energy balance, compared with ordinary structures, the hysteretic energy and hysteretic energy ratio are smaller when a single-layer latticed dome reaches the ultimate limit state, indicating that the plasticity of the members is not fully developed. Therefore, the equivalent pseudo-velocity of input energy, V_E, can be considered as a seismic design parameter because the energy dissipation of the single-layer latticed dome mainly depends on the viscous damping other than hysteretic damping. The decrease of joint rigidity results in the reduction of the hysteretic energy dissipation.

• The dynamic demands are sensitive to the damping ratios. The increase of damping in a structure is favorable for stability. The viscous damping is the main energy dissipation source, which is associated with the non-yielding mechanisms, thus, the correct selection of the viscous damping ratio becomes very important, which rests with carefully considering whether all energy dissipation sources are captured in the dynamic analysis.

Acknowledgments

The research described in this paper was financially supported by the Natural Science

Foundation of China (Grant Nos.: 51108301 and 51078259) and Program for New Century Excellent Talents in University (Grant No.: NCET10-0613).

References

Akiyama, H. (2010), *Earthquake-resistant design method for buildings based on energy balance*, Tsinghua University Press, Beijing, China. (In Chinese)

Bălut, N. and Gioncu, V. (2000), "The influence of geometrical tolerances on the behaviour of space structures", *International Journal of Space Structures*, **15**(3-4), 189-194.

Budiansky, B. and Roth, S. (1962), "Axis-symmetric dynamic buckling of clamped shallow spherical shells", *NASA Technical Note, D-510*, 597-606.

Chadwell, C. (1998), *UCFyber cross section analysis software for structural engineers*, University of California, Berkeley.

Charney, F.A. (2008), "Unintended consequences of modeling damping in structures", *Journal of Structural Engineering*, **134** (4), 581-592.

Charney, F.A. and McNamara, R.J. (2008), "A method for computing equivalent viscous damping ratio for structures with added viscous damping", *Journal of Structural Engineering*, **134** (1), 32-44.

Clough, R.W. and Penzien, J. (1995), *Dynamics of Structures (Third Editon)*, Computers and Structures, Inc., Berkeley, California.

CSI (2006), *PERFORM 3D: Nonlinear Analysis and Performance Assessment for 3D Structures-User Guide (Version 4)*, Computers and Structures, Inc., Berkeley, California.

Dulácska, E. and Kollár, L. (2000), "Buckling analysis of reticulated shells", *Int. J. Space Struct.*, **15**(3-4), 195-203.

El-Tawil, S. and Deierlein, G. (2001a), "Nonlinear analysis of mixed steel-concrete frames. I: element formulation", *J. Struct. Eng.*, **127** (6), 647-655.

El-Tawil, S. and Deierlein, G. (2001b), "Nonlinear analysis of mixed steel-concrete frames. II: implementation and verification", *J. Struct. Eng.*, **127** (6), 656-665.

Fan, F., Cao, Z.G. and Cui, M.Y. (2009), "Elasto-plastic stability of semi-rigidity joint single-layer reticulated domes", *Chinese Journal of Harbin Institute of Technology*, **41**(4), 1-6. (In Chinese)

Gaetano, M. (2001), "Evaluation of seismic energy demand", *Earthq. Engng. Struct. Dyn.*, **30**(4), 485-499.

Gioncu, V. (1995), "Buckling of reticulated shells: state-of-the-art", *Int. J. Space Struct.*, **10**(1), 1-46.

Hiyama, Y., Takashima, H., Iijima, T. and Kato, S. (2000), "Buckling behavior of aluminum ball jointed single layered reticular domes", *Int. J. Space Struct.*, **15**(2), 81-94.

Kato, S., Mutoh, I. and Shomura, M. (1998), "Collapse of semi-rigidly jointed reticulated domes with initial geometric imperfections", *J. Construct. Steel Res.*, **48**(2), 145-168.

Kim, S.D., Kang, M.M. and Kwun, T.J. (1997), "Dynamic instability of shell-like shallow trusses considering damping", *Computer and Structures*, **64**(1-4), 481-489.

Kim, Y.J., Lee, Y.H. and Kim, H. (2008), "Bending test of welded joints for single-layer latticed domes", *Steel Structures*, **8**(4), 357-367.

Li, Q.S. and Chen, J.M. (2003), "Nonlinear elasto-plastic dynamic analysis of single-layer reticulated shells subjected to earthquake excitation", *Computer and Structures*, **81**(4), 177-188.

Li, Z.X. and Shen, Z.Y. (2001), "Shaking table tests of two shallow reticulated shells", *International Journal of Solids and Structures*, **38**(44-45), 7875-7884.

Lopez, A., Puente, I. and Serna, M.A. (2007a), "Direct evaluation of the buckling loads of semi-rigidly jointed single-layer latticed domes under symmetric loading", *Engineering Structures*, **29**(1), 101-109.

Lopez, A., Puente, I. and Serna, M.A. (2007b), "Numerical model and experimental tests on single-layer latticed domes with semi-rigid joints", *Computers and Structures*, **85**(7-8), 360-374.

Masayoshi, N., Mutsuro, S., Yoshio, T. and Osamu, H. (2003), "Structural concept, design and construction of sapporo dome", *International Journal of Steel Structures*, **3**(1), 53-63.

Moghaddam, H.A. (2000), "Seismic behaviour of space structures", *Int. J. Space Struct.*, **15**(2), 119-135.
Nie, G.H. (2003), "On the buckling of imperfect squarely-reticulated shallow spherical shells supported by elastic media", *Thin-Walled Structures*, **41**(1), 1-13.
National Earthquake Hazards Reduction Program (NEHRP). (2010), *Nonlinear Structural Analysis for Seismic Design: A Guide for Practicing Engineers, NEHRP Seismic Design Technical Brief No. 4*, National Institute of Standards and Technology (NIST), U.S. Department of Commerce.
Yuan, X.F. and Dong, S.L. (2002), "Nonlinear analysis and optimum design of cable domes", *Engineering Structures*, **24**(7), 965-977.
Zhang, H.D. and Wang, Y.F. (2012). "Energy-based numerical evaluation for seismic performance of a high-rise steel building", *Steel and Composite Structures*, **13**(6), 501-519.
Zhi, X.D., Fan, F. and Shen, S.Z. (2007), "Failure mechanisms of single-layer reticulated domes subjected to earthquakes", *Journal of the International Association for Shell and Spatial Structures*, **48**(1), 29-44.